GEOPHYSICAL RESEARCH LETTERS, VOL. 23, NO. 14, PAGES 1845-1848, JULY 1, 1996

Axial temperature gradients in dielectric samples in the laser-heated diamond cell

Michael Manga[1] and Raymond Jeanloz

Department of Geology and Geophysics, University of California, Berkeley

Abstract. Temperature gradients inside the laser-heated diamond cell are not measured in the axial direction, along the optic axis, yet can bias estimates of the peak temperatures achieved in optically thin (dielectric) samples such as Mg-silicate perovskite. Thermal diffusion calculations show that the observed thermal-radiation spectrum is not significantly affected by axial temperature gradients. The apparent (measured) temperature underestimates the actual peak sample temperature by 350-850 K for $4000 < T < 6000$ K.

Introduction

The laser-heated diamond cell allows temperatures and pressures typical of the Earth's deep interior to be reproduced under sustained conditions in the laboratory. Large temperature gradients can exist within the sample, however, and could bias measurements and their interpretation [*Heinz and Jeanloz*, 1987a; *Bodea and Jeanloz*, 1989]. This is a concern because accurate temperature measurements are essential to determining melting points and other thermophysical quantities. Recent disagreements in melting temperatures heighten the need to address such potential sources of bias [e.g., *Heinz et al.*, 1994; *Boehler and Zerr*, 1994; *Jeanloz and Kavner*, 1996].

A variety of spectroradiometric techniques have been developed to measure temperatures inside the diamond cell [e.g., *Heinz and Jeanloz*, 1987a; *Boehler et al.*, 1990; *Lazor et al.*, 1993; *Jeanloz and Kavner*, 1996]. Due to the geometry of the experiment (Fig. 1), only the radial distribution of temperature is measured (i.e., temperature variations perpendicular to the optic axis and laser beam). A question thus arises as to the possible biases that may be introduced by temperature variations in the axial direction, parallel to the laser beam.

Two endmember situations can be distinguished. In the case of an opaque (optically thick) sample, such as a metal foil, the sample is typically surrounded by an inert, transparent medium (e.g., Al_2O_3) that contributes little to the emitted thermal radiation. Consequently, the temperature distribution along the top surface of the sample is directly measured, and no significant bias is introduced by axial temperature gradients. In contrast, optically thin materials, such as $(Mg,Fe)SiO_3$ perovskite and other dielectrics, emit comparable amounts of thermal radiation from the entire thickness of the sample. The observed temperature at any point therefore represents an average across the thickness of the sample [*Heinz and Jeanloz*, 1987ab; *Zerr and Boehler*, 1993; *Boehler and Zerr*, 1994]. Here we focus on this second situation, and consider the relationship between the observed temperature and peak temperature for a dielectric sample inside the laser-heated diamond cell.

Axial temperature distribution

The temperature, T, in the sample, diamond, and gasket surrounding the sample, is governed by a diffusion equation

$$\rho C \frac{\partial T}{\partial t} = \nabla \cdot K \nabla T + A \qquad (1)$$

where ρ, C and K are the density, specific heat and thermal conductivity for the region of interest. The absorbed power density A describes heating by the laser, and it is assumed constant throughout the depth of the optically thin sample: the absorption mean-free path for dielectrics is typically $10^{-2} - 100$ cm which is much greater than the sample thickness [e.g., *Fukao et al.*, 1968]. At each interface between two different materials $K\nabla T$ is continuous, and at large distances away from

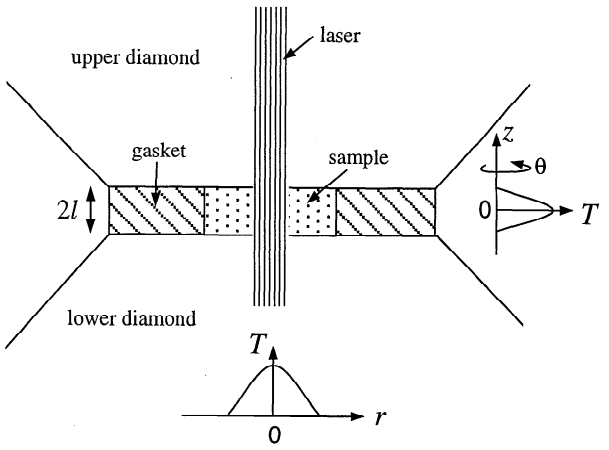

Figure 1. Geometry of the laser-heated diamond cell. The axial or vertical (z) direction is parallel to the laser.

[1] Now at Department of Geological Sciences, University of Oregon, Eugene

Paper number 96GL01602
0094-8534/96/96GL-01602$05.00

the sample the gasket and diamonds are close to room temperature, T_0. The unsteady part of (1), $\rho C \frac{\partial T}{\partial t}$, can typically be ignored because the characteristic diffusive timescale is $O(\rho C l^2/K) \approx 10^{-4}$ s, where $l \approx 10\mu$m is a characteristic dimension of the sample.

The thermal conductivity K is in general a function of temperature, and the effective conductivity can be expressed in the form [e.g., *Schatz and Simmons*, 1974]

$$K_{eff} = K_L + K_R. \tag{2}$$

Here, the lattice (phonon) conductivity K_L and radiative contribution K_R are given by

$$K_L = \frac{K_0}{1 + aT} \quad \text{and} \quad K_R = cT^3 \tag{3}$$

respectively, where a and c may depend on pressure. Although radiative heat transfer may be unimportant for optically thin dielectric samples in the diamond cell, considering the two contributions in (3) allows us to evaluate the possible sensitivity of our results to various temperature dependencies for the thermal conductivity.

If the (sample diameter/sample thickness)$^2 \gg 1$, a condition generally true in the diamond cell, axial gradients are much larger than radial gradients so that (1) reduces to

$$-\frac{\partial}{\partial z} K(T) \frac{\partial T}{\partial z} = A \tag{4}$$

with boundary conditions

$$T = T_0 \text{ at } z = \pm l \text{ and } \partial T/\partial z = 0 \text{ at } z = 0. \tag{5}$$

The second boundary condition in (5) is due to the symmetry of the temperature distribution which, in turn, is due to the sample being optically thin. The conductivity of the diamonds is much greater than that of the sample, so that the diamond-sample interface is close to room temperature, T_0 [*Bodea and Jeanloz*, 1989].

Making the change of variables,

$$s = \int^T K(f) df, \tag{6}$$

equation (4) has the solution

Table 1. Temperature Distribution in Dielectric Samples for Various Conductivity Models

Conductivity model	Temperature distribution
$K = K_0$	$T(z) = T_0 + \frac{Al^2}{2K_0}\left[1 - \left(\frac{z}{l}\right)^2\right]$
$K = cT^3$	$T(z) = \left(T_0^4 + \frac{2Al^2}{c}\left[1 - \left(\frac{z}{l}\right)^2\right]\right)^{1/4}$
$K = \frac{K_0}{(1+aT)}$	$T(z) = \frac{1}{a}\left[(1 + aT_0)e^{\frac{Al^2}{2K_0}\left[1-\left(\frac{z}{l}\right)^2\right]} - 1\right]$

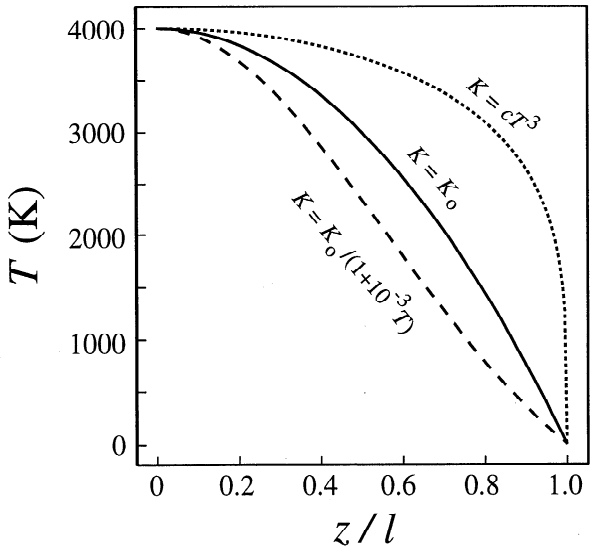

Figure 2. Temperature distributions in the sample for different models of the thermal conductivity; l is the half-thickness of the sample.

$$s(z) = \frac{Al^2}{2}\left[1 - \left(\frac{z}{l}\right)^2\right]. \tag{7}$$

Thus, we can determine the steady-state temperature distribution for different models of the thermal conductivity: see Fig. 2 and Table 1.

Detailed three-dimensional calculations, in which heat transfer in the sample, gasket and diamonds are considered, indicate that the axial temperature distribution is indeed parabolic, as predicted by (7), at all radial positions for K = constant [*Bodea and Jeanloz*, 1989].

Effect of axial temperature gradients on spectroradiometry

For an optically thin sample, the spectroradiometer measures a depth-averaged intensity

$$I(\lambda) = \int_{-l}^{l} L_p[\lambda, T(z)] dz \tag{8}$$

where λ is the wavelength of the light. Here, L is the intensity described by Planck's law

$$L_p(\lambda, T) = \frac{2\pi c^2 h \epsilon}{\lambda^5 (e^{hc/\lambda kT} - 1)} \tag{9}$$

where ϵ, h, k and c are emissivity, Planck's constant, Boltzmann's constant and velocity of light, respectively. We solve (8) numerically for the various temperature distributions given in Table 1 and ϵ = constant, and then determine the apparent sample temperatures corresponding to the integrated light intensities measured by the spectroradiometer.

In practice, the sample temperature is often determined from experimental data by a least-squares fit to the relation [*Jeanloz and Heinz*, 1984]

$$J = \ln \epsilon - \omega T^{-1} \tag{10}$$

where ω is a normalized frequency given by

$$\omega = \frac{hc}{k\lambda} \tag{11}$$

and J is a normalized intensity

$$J = \ln(L_w \lambda^5 / 2\pi c^2 h). \tag{12}$$

Equation (12) is related to temperature through Wien's law

$$L_w(\lambda, T) = \frac{2\pi c^2 h \epsilon}{\lambda^5 e^{hc/\lambda k T}} \tag{13}$$

which is a good approximation to Planck's law for temperatures below 6000 K [*Heinz and Jeanloz*, 1987a]. Use of (10) in analyzing spectroradiometer data provides a convenient means of verifying that a blackbody-like spectrum has been collected by checking the linearity of J as a function of ω; T^{-1} is obtained directly from the slope.

Remarkably, even though large temperature gradients exist across the sample, a graph of J vs ω yields nearly a straight line (see inset of Fig. 3). That is, the wavelength dependence of the vertically integrated light intensity closely follows a Wien (or Planck) distribution with a well determined apparent temperature. In detail, small but systematic deviations from a straight line result in an *apparent* wavelength dependence of emissivity (Fig. 3). Thus, a greybody is expected to exhibit mild non-greybody behavior when one examines the depth-averaged thermal radiation from the diamond cell. We find that an ~25% increase in apparent emissivity from wavelengths of 400 to 900 nm is typical for the integrated light emitted from a dielectric sample, independent of the peak temperature for $1000 < T < 6000$ K.

Note that the absolute magnitude of the apparent emissivity, as measured from the integrated thermal radiation, is characteristically a factor of 2-5 times lower than the actual (intrinsic) emissivity determined from the optical properties of the sample. This is understandable since only a fraction of the sample is contributing significantly to the thermal radiation at the apparent temperature (much of the sample is at lower temperatures). Consequently, the magnitude of the observed greybody emissivity depends on the detailed temperature distribution within the sample. It is for this reason that biases could enter into comparing results from different experimental configurations.

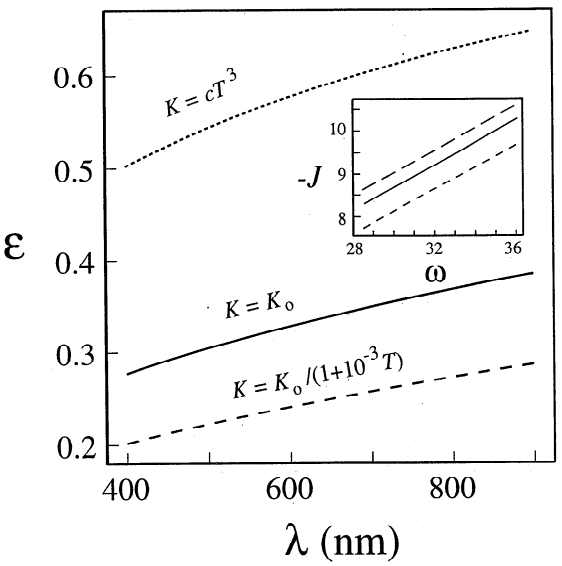

Figure 3. Calculated wavelength dependence of emissivity, normalized by the sample's true greybody emissivity, for different conductivity models. Inset: A plot of $-J$ vs ω is a straight line with a slope of T^{-1}_{measured}; ω in 10^3 K.

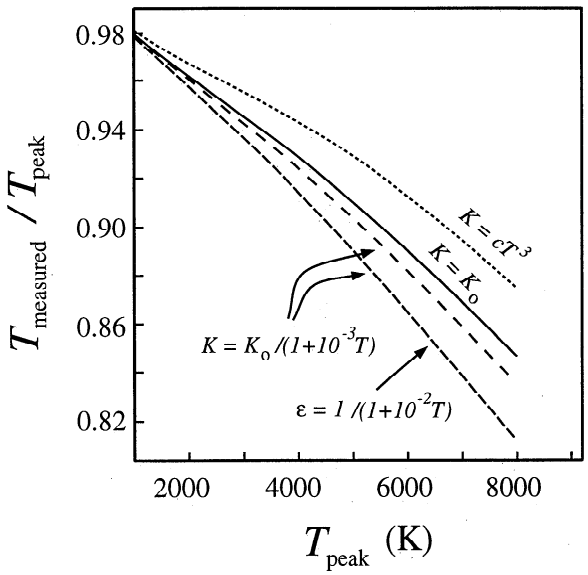

Figure 4. Relationship between the measured temperature, T_{measured}, and the actual peak temperature, T_{peak}, for different conductivity models. The three uppermost curves assume constant emissivities. The lower curve is for a sample with a temperature dependent emissivity and thermal conductivity: $\epsilon = 1.0/(1 + 0.01T)$.

Fig. 4 summarizes the relationship between the apparent temperature, measured from radiated light intensities at 600 nm $< \lambda <$ 900 nm, and the peak sample temperature for different conductivity models. At 4000 K, the measured temperature is $\approx 5 - 10\%$ lower than the actual peak temperature. This result is in good agreement with the calculations of *Heinz and Jeanloz* [1987a] (see their Fig. 14). Moreover, the scaling of the solution (7) ensures that the bias introduced by axial temperature gradients is independent of l.

The emissivity may also be a function of temperature. For example, *Heinz and Jeanloz* [1987b] found that the emissivity of perovskite changes by more than one order of magnitude over a temperature range of 1000 K. Therefore, we also show the apparent sample temperature for a case in which both the conductivity and emissivity are temperature dependent (Fig. 4). Even a strong temperature dependence of emissivity, $\epsilon = 1.0/(1 + 0.01T)$ compatible with the *Heinz and Jeanloz* [1987b] results, has little effect on the measured temperature, however.

The measured temperature, T_{measured}, is always lower than the actual peak temperature, T_{peak}, since much of the sample is at cooler temperatures and provides a measurable contribution to the intensity. The average sample temperature, $\bar{T}$, can be defined as the value obtained from the total light intensity emitted from a region large enough to contain the heated volume; that is, it represents both a radial and axial average of the temperature distribution [*Heinz and Jeanloz*, 1987a]. The effect of vertical temperature gradients on $(T_{\text{measured}} - T_{\text{peak}})/T_{\text{peak}}$ determined here is approximately 1/2 the effect of horizontal gradients on $(\bar{T} - T_{\text{peak}})/T_{\text{peak}}$ determined by *Heinz and Jeanloz* [1987a]. This conclusion agrees with geometrical considerations, which suggest that biases due to temperature gradients in the two horizontal dimensions should be twice as large as the bias due to gradients in the one vertical dimension.

Summary

The relationship between the measured (apparent) temperature and the actual peak temperature within the sample depends only weakly on the temperature dependence of the thermal conductivity and emissivity, and depends most strongly on the sample temperature. A fit of a second order polynomial to our results calculated for a constant conductivity for $1000 < T_{\text{peak}} < 7000$ K (Fig. 4) gives

$$T_{\text{peak}} \approx 0.98 T_{\text{measured}} + 2.7 \times 10^{-5} T^2_{\text{measured}}. \quad (14)$$

Equation (14) can be used to approximately correct measured temperature profiles for dielectric samples heated in a configuration similar to that illustrated in Fig 1. The correction amounts to 350-850 K for measured temperatures in the range of 4000-6000 K. As noted in the introduction, for experiments in which a metal foil is heated by the laser [e.g., *Shen and Lazor*, 1995], the surface temperature of the opaque sample is measured directly. Thus, biases due to temperature gradients, which are inherent in certain experimental configurations, are smaller than the range of temperatures inferred in recently published discrepant melting studies [*Zerr and Boehler* 1993; *Heinz et al.*, 1994; *Boehler and Zerr*, 1994; *Shen and Lazor*, 1995].

Acknowledgments. Comments by J. Nguyen and three reviewers improved this paper. Supported by NSF, NASA, and the Miller Institute for Basic Research in Science.

References

Bodea, S., and R. Jeanloz, Model calculations of the temperature distribution in the laser-heated diamond cell, *J. Appl. Phys., 65*, 4688-4692, 1989.

Boehler, R., and A. Zerr, High-pressure melting of (Mg,Fe)SiO_3-perovskite, *Science, 264*, 280-281, 1994; correction, *ibid, 265*, 723, 1994.

Boehler, R., N. von Bargen, and A. Chopelas, Melting, thermal expansion, and phase transitions of iron at high pressures, *J. Geophys. Res., 95*, 21,731-21,736, 1990.

Fukao, Y., H. Mizutani, and S. Uyeda, Optical absorption spectra at high temperatures and radiative thermal conductivity of olivines, *Phys. Earth Planet. Int., 1*, 57-62, 1968.

Heinz, D.L., and R. Jeanloz, Temperature measurements in the laser-heated diamond cell, in *High-pressure research in mineral physics*, edited by M. Manghnani and Y. Syono, pp. 113-127, American Geophysics Union, Washington, DC, 1987a.

Heinz, D.L., and R. Jeanloz, Measurement of the melting curve of (Mg,Fe)SiO_3 at lower mantle conditions and its geophysical implications, *J. Geophys. Res., 92*, 11,437-11,444, 1987b.

Heinz, D.L., E. Knittle, J.S. Sweeney, Q. Williams, and R. Jeanloz, High-pressure melting of (Mg,Fe)SiO_3-perovskite, *Science, 264*, 279-280, 1994.

Jeanloz, R., and D.L. Heinz, Experiments at high temperature and pressure: Laser heating through the diamond cell, *J. Physique, 45*, 83-92, 1984.

Jeanloz, R., and A. Kavner, Melting criteria and imaging spectroradiometry in laser-heated diamond-cell experiments, *Phil. Trans. Roy. Soc. Lond.*, in press, 1996.

Lazor, P., G. Shen, and S.K. Saxena, Laser-heated diamond anvil cell experiments at high pressure - Melting curve of nickel up to 700 kbar, *Phys. Chem. Minerals, 20*, 86-90, 1993.

Saxena, S.K., G. Shen, and P. Lazor, Temperatures in Earth's core based on melting and phase transformation experiments on iron, *Science, 264*, 405-407, 1994.

Schatz, J.F., and G. Simmons, Thermal conductivity of Earth materials at high temperatures, *J. Geophys. Res., 77*, 6966-6983, 1972.

Shen, G., and P. Lazor, Measurements of melting temperatures of some minerals under lower mantle pressures, *J. Geophys. Res., 100*, 17,699-17,713, 1995.

Zerr, A., and R. Boehler, Melting of (Mg,Fe)SiO_3-perovskite to 625 kilobars: Indication of a high melting temperature in the lower mantle, *Science, 262*, 553-555, 1993

Michael Manga, Department of Geological Sciences, University of Oregon, Eugene, OR 97403

Raymond Jeanloz, Department of Geology and Geophysics, University of California, Berkeley, CA 94720

(received September 8, 1995; revised December 26, 1995; accepted February 28, 1996.)